Paper
Int'l J. of Aeronautical & Space Sci. 17(4), 455–466 (2016)
DOI: http://dx.doi.org/10.5139/IJASS.2016.17.4.455

IJASS
International Journal of Aeronautical and Space Sciences

Expansion of the equilibrium constants for the temperature range of 300K to 20,000K

Jae Gang Kim*

Department of Aerospace System Engineering, Sejong University, Seoul 05006, Republic of Korea

Abstract

Chemical-kinetic parameters of the equilibrium constants to evaluate the reverse rate coefficients in the shock layer of a blunt body and the expanding flows are derived for the temperature range from 300 K to 20,000 K. The expanded equilibrium constants for the chemical reactions of the dissociation, ionization, associative ionization, and neutral and charge exchange reactions of the atmospheric species and carbon materials are proposed in the present work. In evaluating the equilibrium constants, the inter-nuclear potential energies of the molecular species are calculated by the analytical potential function of the Hulburt-Hirschfelder model, and the parameters of the analytical model are determined from the semi-classically calculated RKR potentials. The electronic states and energies of the atoms are calculated by the electronic energy grouping model, and the rovibrational states and energies of each electronic states of the molecules are evaluated by the WKB method. The expanded equilibrium constants for 31 types of the reactions are provided for the best curve-fit functions, and the recombination reaction rate coefficients evaluated from the present equilibrium constants are compared with existing measured values.

Key words: Equilibrium constants, Reverse rate coefficients, Chemical kinetic parameters, Hypersonic Aerothermodynamics

1. Introduction

In the scramjet flight and the ground facility of the shock tunnel to test the hypersonic vehicle aerodynamics, the free-stream and the flight speed range of the vehicle is 2 *km/s*-4 *km/s*, and the corresponded flow-field enthalpy and temperature are 4 *MJ/kg*-8 *MJ/kg* and 1,000 K-20,000 *K*, respectively. In these flow enthalpy and temperature ranges, the nonequilibrium chemical reactions of the dissociation, ionization, associative ionization, and neutral and charge exchange reactions of the atmospheric species and the carbon materials occurs by coupling with the electron-electronic-vibrational nonequilibrium. In the cooling environment of the expanding flows of the shock-tunnel, the reverse chemistry of the recombination dominantly occurs because the temperature of the flow field is below 3,000 *K*. One reason for the difficulty in predicting the heating and cooling environments for such flow-fields is that the unknown of the chemical kinetic parameters and its accuracy in the thermochemical nonequilibrium processes. The best estimate of the chemical kinetic parameters were assessed and tabulated in the works by Park et al.[1-4], Wright et al.[5,6], and Kim et al.[7] These chemical kinetic parameters have been adopted in the popular nonequilibrium hypersonic calculations. However, the chemical parameters of the equilibrium constants proposed in the previous works[1,2] are optimized in a high-temperature environment, above 3,000 *K*. In analyzing the shock boundary layer flows of the scramjet vehicle and the ground test equipment of the shock tunnel, where the temperature of the flow field is below 3,000 *K*, the previous equilibrium constants optimized in the high temperature flow field are inaccurate in analyzing the recombination and the reverse chemical reaction dominant flows.

Towards this end, the equilibrium constants to evaluate the reverse rate coefficients in the shock layer of a blunt body, and the expanding flows are derived for the temperature

* Assistant Professor, Corresponding author: jaegkim@sejong.ac.kr

Received: May 9, 2016 Revised: October 27, 2016 Accepted: October 31, 2016

http://ijass.org pISSN: 2093-274x eISSN: 2093-2480

range of 300 *K* to 20,000 *K*. This temperature range covers the heating and cooling environments of the scramjet flight and expanding flows of the ground facility of shock tunnel. In the present work, the equilibrium constants to evaluate the reverse rate coefficients for the 31 types of the dissociation, ionization, associative ionization, and neutral and charge exchange reactions for the atmospheric species and carbon materials are determined using the best available techniques. In calculating the equilibrium constants, the inter-nuclear potential energies of the molecular species are described by the analytical potential function of the Hulburt-Hirschfelder (H-H) model[8] and the parameters of the analytical models are determined from the semi-classically calculated Rydberg, Klein, and Rees (RKR) potentials[9]. The electronic states and energies of the atoms are calculated by the electronic energy grouping model[10], and the rovibrational states and energies of each electronic state of the molecules are evaluated by the Wentzel, Kramers, and Brillouin (WKB) method[11] based on the present H-H potentials. The expanded equilibrium constants for the 31 types of reactions are provided for the best curve-fit functions, and the reverse reaction rate coefficients evaluated from the present equilibrium constants are compared with the existing measured values for the recombination processes. In nozzle expanding flow calculations, the recombination rates calculated by the present equilibrium constants are also compared with those of the previous equilibrium constants.

2. Atomic and molecular energy database

In the present work, the major 18 chemical species of the neutral and charged particles composing the hypersonic boundary layer are chosen to evaluate the equilibrium constants.

In atoms, four neutrals and its charged species of C, N, O, H, C^+, N^+, O^+, and H^+ of the atmospheric gas and carbon materials are employed to calculate the equilibrium constants. In order to consider the available electronic states and energies of the neutral atomic species, the electronic energy grouping model[10] is adopted in the present work. In the energy grouping model of neutral species, the maximum principle quantum number of n=10 is employed and each electronic states and energies are tabulated in Tables 1 and 2. Such an electronic grouping model was validated in the non-Boltzmann radiation calculations of CN[12] and NO[13], and this grouping model is useful in reducing the computational resources without losing the characteristics of the electronic

Table 1. Electronic states and energies of C and N atoms

Species	n	E_i (cm-1)	g_i	Species	n	E_i (cm-1)	g_i
C	2	30.0	9	N	2	0.0	4
	2	10194.0	5		2	19228.0	10
	2	21648.0	1		2	28840.0	6
	3	60373.0	9		3	83337.0	12
	3	61982.0	3		3	87488.0	18
	3	70387.0	27		3	95276.0	36
	3	71512.0	9		3	96793.0	18
	4	78184.0	12		4	103862.0	18
	3	78472.0	45		3	104857.0	60
	3	78287.0	15		3	104902.0	30
	4	80866.0	36		4	107082.0	54
	4	83846.0	60		5	110021.0	18
	5	83883.0	12		4	110315.0	90
	4	84107.0	84		4	110486.0	126
	5	85037.0	36		5	111363.0	54
	5	86379.0	60		5	112851.0	90
	5	86510.0	192		5	112929.0	288
	6	87713.0	432		6	114298.0	648
	7	88639.0	588		7	115107.0	882
	8	89158.0	768		8	115631.0	1152
	9	89517.0	972		9	115991.0	1458
	10	89779.0	1200		10	116248.0	1800

DOI: http://dx.doi.org/10.5139/IJASS.2016.17.4.455

energy distributions. In charged species, the energy grouping model is unavailable, and the state-of-art electronic states obtained from the NIST database[14] are employed in the present work.

In molecules, the atmospheric species and carbon materials of C_2, CN, CO, N_2, NO, O_2, H_2, N_2^+, NO^+, and O_2^+ are considered in the present work. The major species in the shock layer of a hypersonic vehicle are C, H, O, H_2, C_2, CO, CN, C^+, and H^+. Therefore, at least these species must be accounted for in the calculation of the equilibrium constants. In addition, NO, NO^+, O_2^+, and N_2^+ are employed because NO, NO^+ and O_2^+ have an important role in the nonequilibrium chemical reactions of the atmospheric gas and carbon materials[1], and N_2^+ radiates strongly in the shock layer. In each neutral and charged species, it is difficult to employ the all electronic excited states of molecules because the spectral data is insufficient to evaluate the potentials. In the present work, the available existing spectral data of molecular species of ω_e, $\omega_e x_e$, α_e, B_e, and r_e are adopted from the NIST database[15], and its electronic states are tabulated

Table 2. Electronic states and energies of O, H, C^+, N^+, O^+, and H^+ atoms

Species	n	E_i (cm-1)	g_i	Species	n	E_i (cm-1)	g_i
O	2	78.0	9	H	1	0.00	2
	2	15868.0	5		2	82259.10	8
	2	33792.0	1		3	97492.30	18
	3	73768.0	5		4	102824.00	32
	3	76795.0	3		5	105292.00	50
	3	86629.0	15		6	106632.00	72
	3	88631.0	9		7	107440.00	98
	4	95757.0	8		8	107965.00	128
	3	97445.0	40		9	108325.00	162
	4	99313.0	24		10	108582.00	200
	5	102227.0	8				
	4	102881.0	96				
	5	103869.0	24				
	5	105394.0	168				
	6	106639.0	288				
	7	107583.0	392				
	8	108117.0	512				
	9	108478.0	648				
	10	108734.0	800				
C+	NIST database [14]			N+	NIST database [14]		
O+	NIST database [14]			H+	NIST database [14]		

Table 3. Electronic states of molecules

Species	Electronic states
C_2	$X^1\Sigma_g^+$ $a^3\Pi_u$ $b^3\Sigma_g^-$ $A^1\Pi_u$ $c^3\Sigma_u^+$ $d^3\Pi_g$ $C^1\Pi_g$ $e^3\Pi_g$ $d^1\Sigma_u^+$ $E^1\Sigma_g^+$ $f^3\Sigma_g^-$
CN	$X^2\Sigma^+$ $A^2\Pi$ $B^2\Sigma^+$ $D^2\Pi$ $E^2\Sigma^+$ $F^2\Delta$
CO	$X^1\Sigma^+$ $a^3\Pi$ $a'^3\Sigma^+$ $d^3\Delta$ $e^3\Sigma^-$ $A^1\Pi$ $I^1\Sigma^-$ $D^1\Delta$ $b^3\Sigma^+$ $B^1\Sigma^+$ $C^1\Sigma^+$ $E^1\Pi$ $F^1\Sigma^+$ $G^1\Pi$
N_2	$X^1\Sigma_g^+$ $A^3\Sigma_u^+$ $B^3\Pi_g$ $W^3\Delta_u$ $B'^3\Sigma_u^-$ $a'^1\Sigma_u^-$ $a^1\Pi_g$ $w^1\Delta_u$ $A'^5\Sigma_g^+$ $G^3\Delta_g$ $C^3\Pi_u$ $b^1\Pi_u$ $b'^1\Sigma_u^+$
NO	$X^2\Pi$ $a^4\Pi$ $A^2\Sigma^+$ $B^2\Pi$ $b^4\Sigma^-$ $C^2\Pi$ $D^2\Sigma^+$ $B'^2\Delta$ $E^2\Sigma^+$ $F^2\Delta$ $H^2\Sigma^+$ $H'^2\Pi$
O_2	$X^3\Sigma_g^-$ $a^1\Delta_g$ $b^1\Sigma_g^+$ $c^1\Sigma_u^-$ $A'^3\Delta_u$ $A^3\Sigma_u^+$ $B^3\Sigma_u^-$
H_2	$X^1\Sigma_g^+$ $B^1\Sigma_u^+$ $C^1\Pi_u$ $E^1\Sigma_g^+$ $B'^1\Sigma_u^+$
N_2^+	$X^2\Sigma_g^+$ $A^2\Pi_u$ $B^2\Sigma_u^+$ $D^2\Pi_g$ $C^2\Sigma_u^+$
NO^+	$X^1\Sigma^+$ $a^3\Sigma^+$ $b^3\Pi$ $w^3\Delta$ $b'^3\Sigma^-$ $A'^1\Sigma^+$ $W^1\Delta$ $A^1\Pi$
O_2^+	$X^2\Pi_g$ $a^4\Pi_u$ $A^2\Pi_u$

in Table 3. In evaluating the electronic and rovibrational states and energies of each molecular species, the inter-nuclear potentials are represented in an analytical potential function of H-H model[8], and the form of this H-H model is

$$V(r) = D\left[\left(1-e^{-a(r-r_e)}\right)^2 + ca^3\left(r-r_e\right)^3 e^{-2a(r-r_e)}\left(1+ab\left(r-r_e\right)\right)\right] \quad (1)$$

where r is the inter-nuclear distance, r_e is the equilibrium distance, and D is the potential well depth. In Eq. (1), the potential parameters a, b, and c of each electronic state are determined from a curve-fit of the semi-classically calculated RKR potential[9]. In highly-excited states where the RKR potential is unavailable, the H-H potential parameters are determined as

$$\begin{aligned} a &= \left(\kappa_e / 2D\right)^{\frac{1}{2}} \\ b &= 2 - \frac{1}{c}\left[\frac{7}{12} - \frac{1}{a^2 r_e^2}\left(\frac{5}{4} + \frac{5F}{2} + \frac{5F^2}{4} - \frac{G}{12}\right)\right] \\ c &= 1 - \left(1/ar_e\right)\left(1+F\right) \end{aligned} \quad (2)$$

where the parameters κ_e, F, and G are defined as $\kappa_e = 4\pi^2 c^2 \omega_e \mu$, $F = \alpha_e \omega_e / 6Be^2$ and $G = 8\omega_e x_e / Be$, respectively.

In Fig. 1, the evaluated molecular potential energy curves of each electronic state are compared with the RKR potential energies and existing *ab-initio* calculated energy values for N_2, O_2, CO, and H_2. The *ab-initio* potential energies for the electronic ground state of $N_2(X^1\Sigma_g^+)$, $O_2(X^3\Sigma_u^-)$, $CO(X^1\Sigma^+)$, and $H_2(X^1\Sigma_g)$ were calculated by Jaffe et al.[16,17], Fujita[18], and Schwenke[11] through the best available *ab-initio* calculation packages, respectively. As shown in Fig. 1, the present analytical function of the H-H potential curves of the electronic ground states of N_2, O_2, CO, and H_2 agree with the existing ab-initio calculated values. In comparison with the semi-classical RKR potential energies at low-lying electronic states, it is shown that the present analytical potential energies are also accurately reproduce the semi-classically calculated values for N_2, O_2, CO, and H_2.

In Fig. 2, the evaluated rovibrational states and energies for N_2 and O_2 are presented for the three low-lying

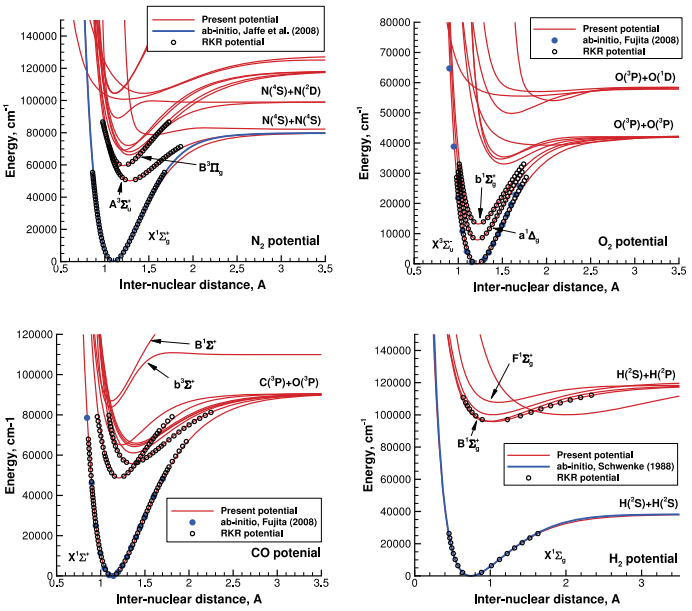

Fig. 1. Inter-nuclear potential energy curves of N_2, O_2, CO, and H_2

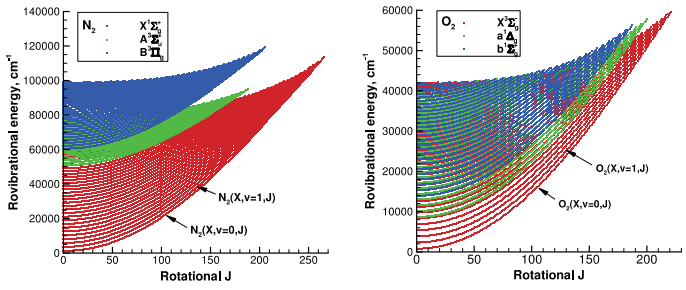

Fig. 2. Rovibrational states and energies of $N_2(X^1\Sigma_g^+, A^3\Sigma_g^+, B^3\Pi_g)$ and $O_2(X^3\Sigma_g^-, a^1\Delta_g, b^1\Sigma_g^+)$

electronic states. In the present work, the rovibrational states and energies in each electronic state are calculated by the WKB method[11] based on the present H-H potential curves. Then, the total number of rovibrational states of N_2 ($X^1\Sigma_g^+$, $A^3\Sigma_g^+$, $B^3\Pi_g$) are 8870, 3359, and 3914 and O_2 ($X^3\Sigma_g^-$, $a^1\Delta_g$, $b^1\Sigma_g^+$) are 5117, 3854, and 3221, respectively. In N_2($X^1\Sigma_g^+$) the maximum vibrational state v_{max} is 60, and the maximum rotational state J_{max} is 266. For electronic ground O_2($X^3\Sigma_g^-$), v_{max} and J_{max} are 36 and 222, respectively. In the present work, the centrifugal distortion due to molecular rotational motion is taken into account in calculating the vibrational states. However, the quasi-bound states of molecules are ignored because they do not significantly affect the heavy-particle impact processes for the temperature range from 300 K to 20,000 K. In the present work, the rovibrational states and energies of C_2, CN, CO, N_2, NO, O_2, H_2, N_2^+, NO^+, and O_2^+ in each electronic available state are evaluated, and this energy database is used in calculating the equilibrium constants.

3. Expansion of the equilibrium constants

In the hypersonic shock layer, the equilibrium temperature is discontinuously increased immediately behind a shock wave, and the internal energy of the electronic, rotational,

Table 4. Types of chemical reactions (*M*=heavy particle)

Type	Reaction channel	Index
Dissociation	$C_2 + M \leftrightarrow C + C + M$	D1
	$CN + M \leftrightarrow C + N + M$	D2
	$CO + M \leftrightarrow C + O + M$	D3
	$N_2 + M \leftrightarrow N + N + M$	D4
	$NO + M \leftrightarrow N + O + M$	D5
	$O_2 + M \leftrightarrow O + O + M$	D6
	$H_2 + M \leftrightarrow H + H + M$	D7
Ionization	$C + e^- \leftrightarrow C^+ + e^- + e^-$	I1
	$N + e^- \leftrightarrow N^+ + e^- + e^-$	I2
	$O + e^- \leftrightarrow O^+ + e^- + e^-$	I3
	$H + e^- \leftrightarrow H^+ + e^- + e^-$	I4
Associative	$O + N \leftrightarrow NO^+ + e^-$	A1
-ionization	$N + N \leftrightarrow N_2^+ + e^-$	A2
	$O + O \leftrightarrow O_2^+ + e^-$	A3
Exchange	$N_2 + O \leftrightarrow NO + N$	E1
-reaction	$NO + O \leftrightarrow O_2 + N$	E2
	$CO + C \leftrightarrow C_2 + O$	E3
	$CO + O \leftrightarrow O_2 + C$	E4
	$CO + N \leftrightarrow CN + O$	E5
	$N_2 + C \leftrightarrow CN + N$	E6
	$CN + O \leftrightarrow NO + C$	E7
	$CN + C \leftrightarrow C_2 + N$	E8
Charge	$N_2 + O_2^+ \leftrightarrow N_2^+ + O_2$	C1
-exchange	$NO^+ + N \leftrightarrow O^+ + N_2$	C2
-reaction	$NO^+ + O \leftrightarrow N^+ + O_2$	C3
	$NO^+ + O_2 \leftrightarrow O_2^+ + NO$	C4
	$NO^+ + N \leftrightarrow N_2^+ + O$	C5
	$O_2^+ + N \leftrightarrow N^+ + O_2$	C6
	$O^+ + NO \leftrightarrow N^+ + O_2$	C7
	$NO^+ + O \leftrightarrow O_2^+ + N$	C8
	$O^+ + N_2 \leftrightarrow N_2^+ + O$	C9

and vibrational energies are relaxed into the equilibrium conditions. In this thermochemical nonequilibrium hypersonic flow field, the forward and reverse chemical reactions of the dissociation, ionization, associative ionization, and neutral and charge exchange reactions occurs coupled with the nonequilibrium conditions of the atomic and molecular internal energies. In cooling environment of the nozzle expanding flows of the shock-tunnel facility, the temperature of the test gas is increased by the reflected shock, and the velocity of the test gas is accelerated through the nozzle expanding flows. In this acceleration processes, the temperature of the gas is rapidly decreased and the reverse reaction of recombination is dominantly occurred. In the reverse reaction processes of the hypersonic shock layer and nozzle expanding flows, the equilibrium constants K_e are adopted to determine the reverse rate coefficients K_r of the recombination and exchange reactions for the neutral and ion. Then, K_r can be determined as

$$K_r(T) = \frac{K_f(T, T_{eev})}{K_e(T)} \tag{3}$$

where K_f is the forward rate coefficients, and T and T_{eev} are the equilibrium temperature and electron-electronic-vibrational temperature, respectively. In the thermochemical nonequilibrium flows, the two-temperature model[19,20] is widely used to determine the forward rate coefficients K_f, and the chemical kinetic parameters of the atmospheric gas and carbon materials were assessed and tabulated in the work by Park et al[1,3]. In the present work, the equilibrium constants K_e are evaluated in the temperature range of 300 K to 20,000 K to accurately describe the reverse chemical reactions of the hypersonic shock layer and the nozzle expanding flows. Thirty-one types of the chemical reactions of the dissociation, ionization, associative ionization, and neutral and charge exchange reactions of the atmospheric species and carbon materials are considered, and such types of the chemical reactions are tabulated in Table 4.

In the dissociation and recombination processes of AB+M → A+B+M for D1 to D7 reaction types, the equilibrium constants are evaluated by the regular Saha equation[19] as

$$K_e(T) = \frac{Q_{t_A} Q_{t_B} \Sigma_e Q_A \Sigma_e Q_B}{Q_{t_{AB}} \Sigma_e \Sigma_v \Sigma_J [Q_{AB} exp(E_D / kT)]} \tag{4}$$

where Q_t is the translational partition function, Q_A and Q_B are the atomic partition functions of the electronic excited states of the A and B atoms, Q_{AB} is the molecular partition function related to the electronic-rovibrational excited states of the AB molecule, and E_D is the reaction energy of dissociation. The translational, atomic, and molecular partition functions were detailed in the non-Boltzmann radiation analysis work by Hyun[10]. In the hypersonic shock layer and nozzle expanding flows, the dissociation and its recombination reactions are dominant chemical reactions. Therefore, the present work employs the state-of-art method to calculate the equilibrium constants for the dissociation and recombination reactions are. In calculating the atomic partition functions, the present electronic energy grouping model and electronic energy database for the neutral and charged atoms are employed. In molecular partition function calculations, the present rovibrational energies evaluated by the WKB method based on the analytical H-H potential functions are adopted.

In the present work, the electronic and rotational-dependent dissociation energy E_D is adopted to determine the equilibrium constants of Eq. (4). In Fig. 3, the dissociation energy in each rotational excited state of the electronic ground N_2 and O_2 are presented. In molecules, the potential energy is distorted by the rotational excitation, and the effective potential needs to be considered to determine the dissociation energy of the rotational excited states. In N_2, the difference of the dissociation energy between J=0 and J=200 is about 1.71 *eV*. In O_2, the difference between the J=0 and J=200 is about 1.64 eV. These differences of the dissociation energy depending on the rotational excitation is too large to adopt the constant dissociation energy model. Therefore, in the present work, the molecular dissociation energy E_D for the C_2, CN, CO, N_2, NO, O_2, and H_2 depending on the rotational states are calculated for each electronic state,

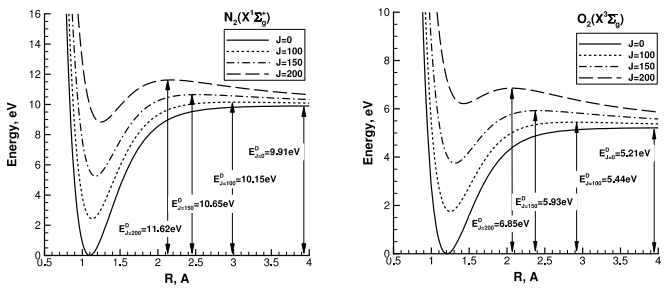

Fig. 3. Dissociation energy of $N_2(X^1\Sigma_g^+)$ and $O_2(X^3\Sigma_g^-)$ for the rotational excited states

and these rotational-dependent dissociation energies are employed to determine the equilibrium constants for the reactions of D1 to D7.

In the ionization and recombination processes of I1 to I4, the equilibrium constants are evaluated by

$$K_e(T) = 2Q_+ \left[\Sigma_i g_i exp\left(\frac{E_{ion} - E_i}{kT} \right) \right]^{-1} \left(\frac{2\pi m_e kT}{h^2} \right)^{1.5} \quad (5)$$

where Q_+ is the atomic partition function of the charged species, m_e is the electron mass, E_{ion} is the ionization energy, and k and h is the Boltzmann and Plank constants, respectively. E_i and g_i are the electronic energy and its multiplicity of ith electronic state. In the present work, the electronic energy grouping model of atom is adopted to determine the electronic energy E_i. The ionization energy of E_{ion} for the atomic species of C, N, O, and H are obtained from the NIST database[14].

In the associative ionization and neutral and charge exchange reaction processes of A+B → C+D for A1 to A3, E1 to E8, and C1 to C9, the equilibrium constants are evaluated by

$$K_e(T) = \frac{Q_{t_C} Q_C Q_{t_D} Q_D}{Q_{t_A} Q_A Q_{t_B} Q_B} exp\left(-\frac{E_R}{kT} \right) \quad (6)$$

where E_R is the reaction energy of the forward chemical reactions. In the present work, the reaction energy E_R of each reaction type is evaluated by the net energy of the species formation enthalpy, and the species formation enthalpy is obtained from the NIST-JANAF thermochemical tables[21].

In Fig. 4, the equilibrium constants evaluated by the present work are compared with the previous equilibrium constants[1] for the dissociation, ionization, exchange reaction, and associative ionization processes. The present equilibrium constants above 3,000 K have identical values with the previous equilibrium constants evaluated by Park[1]. However, except the ionization processes, the equilibrium constants have significant differences with the previous values below 3,000 K. This is because the previous equilibrium constants were optimized for high temperature gases above 3,000 K. In the nozzle expanding flows of the shock-tunnel facility and the hypersonic boundary layer flows near the vehicle surface, the temperature of the flow field is below 3,000 K. In this flow field, the reverse chemical reactions of the recombination and exchange reactions of the atmospheric species and carbon materials dominantly occur, and the accurate equilibrium constants are needed to calculate the best available reverse rate coefficients.

In Fig. 5, the recombination rate coefficients calculated by the present work are compared with the existing measured values[22-46]. In order to calculate the recombination rate coefficients, the best available forward rate coefficients K_f of Eq. (3) of each chemical reaction case are obtained from the assessment and analysis work by Cohen and Westberg[47] and Baulch et al[26]. Then, the theoretical recombination rate coefficients are evaluated by Eq. (3) with the present and previous equilibrium constants[1]. In N_2, recombination reactions, the measured values mostly exist at the low temperatures of about 300 K, and the recombination rate coefficients calculated by the present equilibrium constants

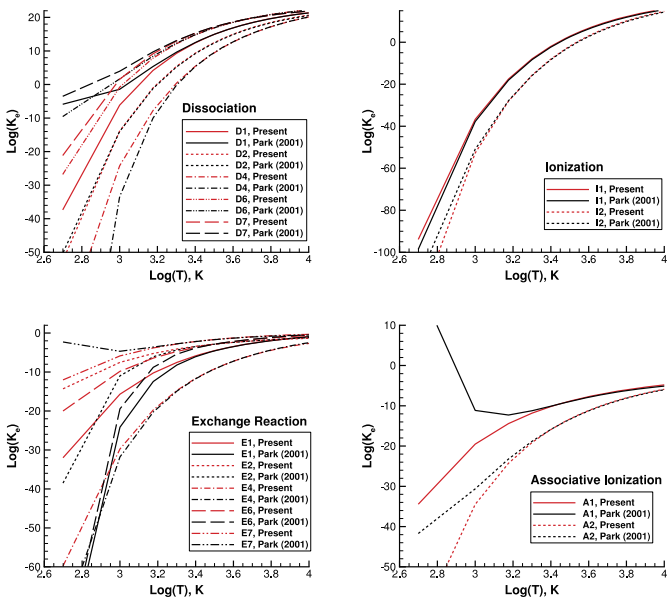

Fig. 4. Comparisons of the present and previous[1] equilibrium constants

can more closely reproduce the experimental measured values than the rate coefficients calculated by the previous equilibrium constants. In O_2 and H_2 recombination reactions, the recombination rate coefficients calculated by the present equilibrium constants can also more closely reproduce the measured rate coefficients for the temperature ranges of 300 *K* to 20,000 *K*. In ionic recombination, both recombination rate coefficients calculated by the present and previous equilibrium constants agree with the measured rate coefficients. However, at low temperatures below 500 K, the recombination rate by the previous equilibrium constants are drastically increased.

In the present work, the equilibrium constants for the dissociation, ionization, associative ionization, and neutral and charge exchange reactions of the atmospheric species and carbon materials are calculated at temperatures from 300 *K* to 20,000 *K*. The resulting values of the 31 types of the reactions are fitted by the expression

$$K_e(T) = exp\left[\frac{A_1}{Z} + A_2 + A_3 lnZ + A_4 Z + A_5 Z^2\right] \quad (7)$$

where Z=10,000/T. The parameters A_1 to A_5 for the reactions are tabulated in Table 5.

4. Sample expanding flow calculation

A one-dimensional space-marching calculation for pure oxygen is performed to determine the properties of the nonequilibrium reacting flows in the nozzle expansions. The geometry has a divergent type of the nozzle with a 2 *m* length, and the area ratio between the nozzle throat and exist is A/A^*=200. The calculation is started at the nozzle inlet with the conditions of Mach number M=1, pressure p=10 *atm*, and the temperature T=1,500 *K*. These initial conditions are available to produce a hypersonic speed of M=8 at the nozzle exist. The initial species mole-fractions of pure oxygen at the nozzle inlet are set to 90%O_2-10%O and 80%O_2-20%O. These ratios are similar to those of the settling chamber conditions of p=10 *atm* and T=1,500 *K*. In the present work, we assume that the heavy-particle translational and rotational temperatures equilibrate in the entire nozzle flow field, and these temperatures are set as an equilibrium temperature T.

The chemical reactions of the forward direction are computed using the two-temperature model[19,20], and the reverse reactions are calculated by using the present and previous equilibrium constants[1]. In order to compare the equilibrium constants in the recombination rates of pure oxygen, only D6 type of reaction in Table 4 is considered in the nozzle expanding flow calculations. The dissociation reactions by heavy-particle impact are controlled by the geometrically averaged temperature $T_a = \sqrt{TT_{eev}}$, and the recombination reactions are controlled by the equilibrium temperature T. Then, the rate of the number density of O2 can be calculated by

$$\omega_{O_2} = \Sigma_m \left[K_{r_m}(T) n_O n_O n_m - K_{f_m}(T_a) n_{O_2} n_m\right] \quad (8)$$

where the subscription m is the collision species index of the heavy-particles of O and O_2. In the present work, the forward rate coefficients K_f is obtained from the work by Park[3], and

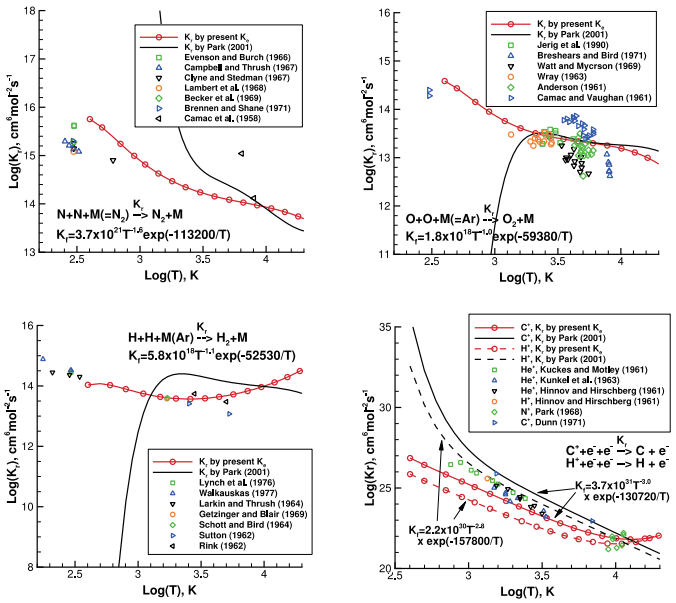

Fig. 5. Comparisons between the measured neutral and ionic recombination rates[22-46] and the theoretically calculated values

the recombination rate coefficients K_r is calculated by Eq. (3) with the present and previous equilibrium constants[1].

To account for the electron-electronic-vibrational nonequilibrium, the Landau-Teller model is employed[19]. In order to compare the equilibrium constants in recombination processes, only the vibrational-translational (V-T) energy transfer is treated in the nozzle expanding flow calculations because the V-T energy transfer is a major energy transition, and it dominantly affects to the dissociation-recombination reactions in the nozzle expanding flows. Then, the V-T energy transfer can be calculated by

$$\frac{dE_{eev}}{dt} = \frac{E^*_{eev}(T) - E_{eev}}{\tau_v} + \phi_v D_{O_2} \omega_{O_2} \tag{9}$$

where E_{eev} is the electron-electronic-vibrational energy, E^*_{eev} is the equilibrium value specified by the equilibrium temperature T, and D_{O_2} is the averaged dissociation energy of O_2. The time τ_v is the sum of the Landau-Teller relaxation time calculated by the expression of Millikan and White[48] and the collision-limited relaxation time[19,20]. In order to maintain the total energy conservation, the vibrational energy loss due to dissociation needs to be considered, and the vibrational energy loss ratio ϕ_v of O_2 is set to 0.3.

In Fig. 6, the results of the nozzle expanding flow calculations are compared with the analytical solutions. In the supper sonic nozzle flows, the analytical solutions of Mach number, pressure, density, and temperature can be calculated through the equations of

Table 5. Parameters of the equilibrium constants

Type	A_1	A_2	A_3	A_4	A_5
D1	-1.1123E+00	3.0777E+00	3.0997E+00	-7.5664E+00	5.3007E-03
D2	-4.0521E-01	2.5479E+00	2.5400E+00	-9.3101E+00	7.4899E-03
D3	1.8537E+00	1.9829E+00	1.9465E+00	-1.3236E+01	5.7902E-03
D4	7.1552E-01	2.4905E+00	2.0911E+00	-1.1686E+01	5.9207E-03
D5	-6.2289E-01	2.0925E+00	2.0277E+00	-7.8722E+00	5.5857E-03
D6	1.2173E+00	1.5665E+00	1.9085E+00	-6.2810E+00	5.2365E-03
D7	-7.0955E-01	1.9278E+00	2.1293E+00	-5.6164E+00	7.4150E-03
I1	-4.1277E+00	-1.3458E+00	-2.4596E+00	-1.2915E+01	-2.5903E-03
I2	-3.0056E+00	-1.2165E+00	-2.3538E+00	-1.6749E+01	-2.1952E-03
I3	-5.3901E+00	-2.6602E-01	-1.7474E+00	-1.5754E+01	-7.6615E-04
I4	-4.8298E+00	-7.7348E-01	-2.1358E+00	-1.5679E+01	-1.8113E-03
A1	-7.9757E+00	1.9066E-01	-1.8480E+00	-3.2553E+00	-1.6617E-03
A2	-6.9094E+00	1.4204E-01	-1.9215E+00	-6.7921E+00	-1.7487E-03
A3	-7.6033E+00	-7.1828E-03	-2.0994E+00	-8.0704E+00	-1.9887E-03
E1	1.7275E+00	-1.7891E-01	-2.1716E-01	-3.7328E+00	-2.2848E-04
E2	-1.3900E+00	-1.6728E-01	-1.6562E-01	-1.5506E+00	-1.1016E-04
E3	-5.2541E-02	-2.1175E-01	-2.5656E-01	-5.7116E+00	-4.7940E-04
E4	1.1620E+00	-3.9818E-01	-3.9796E-01	-6.8677E+00	-5.2734E-04
E5	1.7910E+00	-1.4789E-01	-1.3448E-01	-3.9133E+00	-2.9263E-04
E6	9.6645E-01	-9.5897E-02	-1.1930E-01	-2.3289E+00	-1.0393E-04
E7	7.6102E-01	-8.3008E-02	-9.7862E-02	-1.4038E+00	-1.2454E-04
E8	-1.8436E+00	-6.3857E-02	-1.2208E-01	-1.7983E+00	-1.8677E-04
C1	1.0314E+00	-1.9696E-01	-2.0486E-01	-4.0050E+00	-9.8663E-05
C2	-5.4189E-01	-6.2998E-02	-4.4489E-02	-1.2662E+00	-1.0889E-04
C3	-7.7980E-01	-4.0919E-01	-4.2727E-01	-7.6179E+00	-4.4753E-04
C4	1.7624E+00	-3.0561E-02	-8.5804E-02	-3.2645E+00	-2.1682E-04
C5	1.0663E+00	-4.8620E-02	-7.3502E-02	-3.5368E+00	-8.7011E-05
C6	-1.1521E+00	-2.1134E-01	-1.7584E-01	-2.8028E+00	-1.2054E-04
C7	-1.9654E+00	-1.6728E-01	-1.6562E-01	-2.6190E+00	-1.1016E-04
C8	3.7234E-01	-1.9784E-01	-2.5142E-01	-4.8151E+00	-3.2698E-04
C9	1.6082E+00	1.4378E-02	-2.9013E-02	-2.2706E+00	2.1879E-05

$$\frac{A}{A^*}=\frac{1}{M}\left[\left(\frac{2}{\gamma+1}\right)\left(1+\frac{\gamma-1}{2}M^2\right)\right]^{\frac{\gamma+1}{2(\gamma-1)}} \tag{10}$$

$$p=p_t\left(1+\frac{\gamma-1}{2}M^2\right)^{-\frac{\gamma}{\gamma-1}} \tag{11}$$

$$\rho=\rho_t\left(1+\frac{\gamma-1}{2}M^2\right)^{-\frac{1}{\gamma-1}} \tag{12}$$

$$T=T_t\left(1+\frac{\gamma-1}{2}M^2\right)^{-1} \tag{13}$$

respectively. γ is the specific heat ratio and p_t, ρ_t, T_t are the pressure, density, and temperature at the stagnation conditions. In the analytical solutions, the specific heat ratio is set to constant as 1.4, and the stagnation parameters can be determined from the inlet conditions. In comparisons between the results of the nozzle expanding flow calculations and the analytical solutions, the present results have almost identical with those of the analytical solutions except the Mach number and temperature. In comparisons of the Mach number and temperature, the present results are slightly under or overestimate the analytical solutions. This is because, in the present results, the specific heat ratio γ is not constant, and it depends on the thermochemical nonequilibrium conditions.

In Fig. 7, the comparisons of the species mole-fraction of O and the electron-electronic-vibrational temperature calculated by the present and previous equilibrium constants[1] are presented for the nozzle expanding flows. In the front part of nozzle until x=10 *cm*, the most of atomic O is recombined to O_2, and the electron-electronic-vibrational temperature is ascended up to 2,000 *K* and 2,700 *K* for 90%O_2-10%O and 80%O_2-20%O cases, respectively. This is because the electron-electronic-vibrational energy is added into a flow field by the recombination processes. In the downstream of the nozzle expanding flows after x=10 *cm*, the rarefaction of the density drastically occurs, and the recombination reaction and the electron-electronic-vibrational relaxation rapidly froze. In comparisons of the mole-fraction of O between the present and previous equilibrium constants, the difference of the species mole-fraction of O is obviously shown, even though most chemical reactions are rapidly frozen in the downstream part of the nozzle. The recombination rates calculated by the present equilibrium constants is larger than those of the previous values, and the species mole-fraction of O by the present equilibrium constants is twice less than that by the previous equilibrium constants. The difference of the recombination rates generates the difference of the electron-electronic-vibrational temperature because the recombined species density of O_2 affects the relaxation time of electron-electronic-vibrational energy.

5. Concluding Remarks

To evaluate the reverse rate coefficients in the shock layer

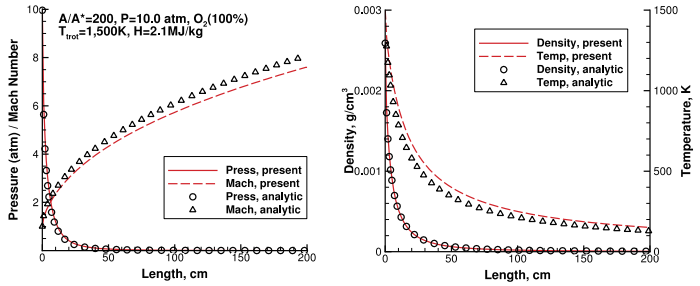

Fig. 6. Results of the nozzle expanding flow calculations

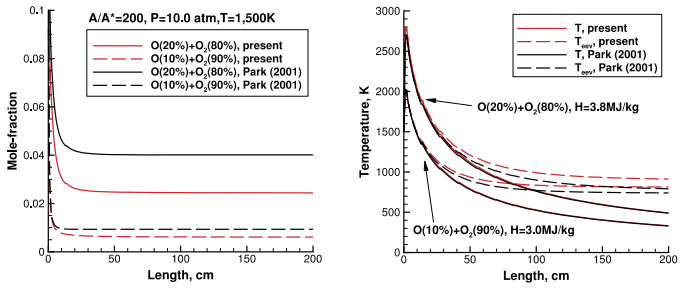

Fig. 7. Comparisons of the results of the nozzle expanding flow calculations between the present and previous[1] equilibrium constants

of a blunt body and the expanding flows, the chemical-kinetic parameters of the equilibrium constants are derived in the temperature range of 300 K to 20,000 K. For C, N, O, H, C^+, N^+, O^+, H^+, C_2, CN, CO, N_2, NO, O_2, H_2, N_2^+, NO^+, and O_2^+, the exact electronic, rotational, and vibrational quantum energies of atoms and molecules are evaluated based on the state-of-art spectral data and the exact potential energy models. The expanded equilibrium constants for the 31 types of the chemical reactions including the dissociation, ionization, associative ionization, and neutral and charge exchange reactions of the atmospheric species and carbon materials are determined using the best available techniques. The present equilibrium constants are provided for the 5-parameter curve-fit function, and the parameters are tabulated in the present work.

Acknowledgement

The author gratefully acknowledges funding for this work through ADD Grant UD150034.

References

[1] Park, C., "Chemical-Kinetic Parameters of Hyperbolic Earth Entry", *Journal of Thermophysics and Heat Transfer*, Vol. 15, No. 1, 2001, pp. 76-90.

[2] Park, C., "On Convergence of Computation of Chemically Reacting Flows", AIAA Paper 85-0247, *Proceedings of the 23rd Aerospace Sciences Meeting*, Reno, NV, 1985.

[3] Park, C., "Review of Chemical-Kinetic Problems of Future NASA Mission. I-Earth Entries", *Journal of Thermophysics and Heat Transfer*, Vol. 7, No. 3, 1993, pp. 385-398.

[4] Park, C., Howe, J. T., Jaffe, R. L. and Candler, G. V., "Review of Chemical-Kinetic Problems of Future NASA Mission. II-Mars Entries", *Journal of Thermophysics and Heat Transfer*, Vol. 8, No. 1, 1994, pp. 9-23.

[5] Wright, M. J., Bose, D., Palmer, G. E. and Levin, E., "Recommended Collision Integrals for Transport Property Computations Part 1: Air Species", *AIAA Journal*, Vol. 43, No.12, 2005, pp. 2558-2564.

[6] Wright, M. J., Hwang, H. H. and Schwenke, D. W., "Recommended Collision Integrals for Transport Property Computations Part II: Mars and Venus Entries", *AIAA Journal*, Vol. 45, No. 1, 2007, pp. 281-288.

[7] Kim, J. G., Kwon, O. J. and Park, C., "A High Temperature Elastic Collision Model for DSMC Based on Collision Integrals", AIAA Paper 2006-3803, P*roceedings of the 9th AIAA/ASME Joint Thermophysics and Heat Transfer Conferenc*e, San Francisco, CA, 2006.

[8] Steele, D., Lippincott, E. R. and Vanderslice, J. T., "Comparative Study of Empirical Internuclear Potential Functions", *Reviews of Modern Physics*, Vol. 34 No. 2, 1962, pp. 239-251.

[9] Vanderslice, J. T., Mason, E. A., Maisch, W. G. and Lippincott, E. R., "Ground State of Hydrogen by the Rydberg-Kelein-Rees Method", *Journal of Molecular Spectroscopy*, Vol. 2, No. 1, 1959, pp. 17-29.

[10] Hyun, S. Y., "Radiation Code SPRADIAN07 and its Applications", Ph. D. Dissertation, Dept. of Aerospace Engineering, Korea Advanced Institute of Science and Technology, Daejeon, Republic of Korea, 2009.

[11] Schwenke, D.W., "Calculations of Rate Constants for the Three-Body Recombination of H_2 in the Presence of H_2", *Journal of Chemical Physics*, Vol. 89, No. 4, 1988, pp. 2076-2091.

[12] Hyun, S. Y., Park, C. and Chang, K. S., "Rate Parameters for Electronic Excitation of Diatomic Molecules: CN Radiation", *Journal of Thermophysics and Heat Transfer*, Vol. 23, No. 2, 2009, pp. 226-235.

[13] Hyun, S. Y., Park, C. and Chang, K. S., "Rate Parameters for Electronic Excitation of Diatomic Molecules: NO Radiation", *Journal of Thermophysics and Heat Transfer*, Vol. 23, No. 4, 2009, pp. 641-650.

[14] NIST atomic spectra database, http://www.nist.gov/pml/data/asd.cfm

[15] NIST molecular spectra database, http://webbook.nist.gov/chemistry

[16] Jaffe, R. L., Schwenke, D. W., Chaban, G. and Huo, W., "Vibrational and Rotational Excitation and Relaxation of Nitrogen from Accurate Theoretical Calculations", *AIAA Paper 2008-1208, Proceedings of the 46th AIAA Aerospace Sciences Meeting*, Reno, NV, 2008.

[17] Jaffe, R. L., Schwenke, D. W. and Chaban, G., "Theoretical Analysis of N2 Collisional Dissociation and Rotation-Vibration Energy Transfer", AIAA Paper 2009-1569, *Proceedings of the 47th AIAA Aerospace Sciences Meeting*, Orlando, Florida, 2009.

[18] Fujita, K., "Vibrational Relaxation and Dissociation Kinetics of CO by CO-O Collisions", AIAA Paper 2008-3919, *Proceedings of 40th Thermophysics Conference*, Seattle, WA, 2008.

[19] Park, C., *Nonequilibrium Hypersonic Aerothermodynamics*, Wiley, New York, 1990.

[20] Park, C., "Assessment of Two-Temperature Kinetic Model for Ionizing Air", *Journal of Thermophysics and Heat Transfer*, Vol. 3, No. 3, 1989, pp. 233-244.

[21] NIST-JANAF Thermochemical Tables, http://kinetics.

nist.gov/janaf/

[22] Evenson, K. M. and Burch D. S., "Atomic-Nitrogen Recombination", *Journal of Chemical Physics*, Vol. 45, No. 7, 1966, pp. 2450-2460.

[23] Campbell, I. M. and Thrush, B. A., "The Recombination of Nitrogen Atoms and the Nitrogen Afterglow", *Proceedings of the Royal Society A*, Vol. 296, 1967, pp. 201-221.

[24] Clyne, M. A. A. and Stedman, D. H., "Rate of Recombination of Nitrogen Atoms", *Journal of Physical Chemistry*, Vol. 71, No. 9, 1967, pp. 3071-3073.

[25] Lambert, R. M., Christie, M. I., Golesworthy, R. C. and Linnett, J. W., "Mass Spectrometric Study of the Reaction of Nitrogen Atoms with Acetaldehyde" *Proceedings of the Royal Society A*, Vol. 302, 1968, pp. 167-183.

[26] Baulch, D. L., Drysdale, D. D. and Horne, D. G., *Evaluated Kinetic Data for High Temperature Reactions*, Vol. 2, CRC Press, London, 1973.

[27] Brennen, W. and Shane, E. C., "Nitrogen Afterglow and the Rate of Recombination of Nitrogen Atoms in the Presence of Nitrogen, Argon, and Helium", *Journal of Physical Chemistry*, Vol. 75, No. 10, 1971, pp. 1552-1564.

[28] Camac, M., Camm, J., Feldman, S., Keck, J. and Petty, C., "Chemical Relaxation in Air, Oxygen and Nitrogen", *Institute of Aeronautical Sciences Preprint No. 802*, New York, 1958.

[29] Jerig, L., Thielen, K. and Roth, P., "High-Temperature Dissociation of Oxygen Diluted in Argon or Nitrogen", *AIAA Journal*, Vol. 29, No. 7, 1990, pp. 1136-1139.

[30] Breshears, W. D. and Bird, P. F., "Density Gradient Measurements of O2 Dissociation in Shock Waves", *Journal of Chemical Physics*, Vol. 55, No. 8, 1971, pp. 4017-4026.

[31] Watt, W. S. and Myerson, A. L., "Atom Formation Rates Behind Shock Waves in Oxygen", *Journal of Chemical Physics*, Vol. 51, No. 4, 1969, pp. 1638-1643.

[32] Wray, K. L., "Shock-Tube Study of the Recombination of O Atoms by Ar Catalysts at High Temperatures", *Journal of Chemical Physics*, Vol. 38, No. 7, 1963, pp. 1518-1524.

[33] Anderson, O. L., "Shock-Tube Measurement of Oxygen Dissociation Rate in Argon", United Aircraft Corporation Research Laboratories, Report R-1828-1,1961.

[34] Camac, M. and Vaughan, A., "O_2 Dissociation Rates O2-Ar Mixtures", *Journal of Chemical Physics*, Vol. 34, No. 2, 1961, pp. 460-470.

[35] Lynch, K. P., Schwab, T. C. and Michael, J. V., "Lyman-α Absorption Photometry at High Pressure and Atom Density Kinetic Results for H Recombination", *International Journal of Chemical Kinetics*, Vol. 8, No. 5, 1976, pp. 651-671.

[36] Walkauskas, L. P. and Kaufman, F., "Gas Phase Hydrogen Atom Recombination", *Symposium (International) on Combustion*, Vol. 15, No. 1, 1975, pp. 691-699.

[37] Larkin, F. S. and Thrush, B. A., "Recombination of Hydrogen Atoms in the Presence of Atmospheric Gases", *Discussions of the Faraday Society*, Vol. 37, 1964, pp. 112-117.

[38] Getzinger, R. W. and Blair, L. S., "Recombination in the Hydrogen-Oxygen Reaction: a Shock Tube Study with Nitrogen and Water Vapour as Third Bodies", *Combustion and Flame*, Vol. 13, No. 3, 1969, pp. 271-284.

[39] Schott, G. L. and Bird, P. F., "Kinetic Studies of Hydroxyl Radicals in Shock Waves. IV. Recombination Rates in Rich Hydrogen-Oxygen Mixtures", *Journal of Chemical Physics*, Vol. 41, No. 9, 1964, pp. 2869-2876.

[40] Sutton, E. A., "Measurement of the Dissociation Rates of Hydrogen and Deuterium", *Journal of Chemical Physics*, Vol. 36, No. 11, 1962, pp. 2923-2931.

[41] Rink, J. P., "Shock Tube Determination of Dissociation Rates of Hydrogen", *Journal of Chemical Physics*, Vol. 36, No. 1, 1962, pp. 262-265.

[42] Kuckes, A. F., Motley, R. W., Hinnov, E. and Hirschberg, J. G., "Recombination in a Helium Plasma", *Physical Review Letter*s, Vol. 6, No. 7, 1961, pp. 337-339.

[43] Kunkel, W. B., Robben, F. and Talbot, L., "Spectroscopic Study of Electron Recombination with Monatomic Ions in a Helium Plasma", *Physical Review 2nd. Series*, Vol. 132, No. 6, 1963, pp. 2363-2371.

[44] Hinnov, E. and Hirschberg, J. G., "Electron-Ion Recombination in Dense Plasmas", *Physical Review*, Vol. 125, No. 3, 1961, pp. 795-801.

[45] Park, C., "Measurement of Ionic Recombination Rate of Nitrogen", *AIAA Journal*, Vol. 6, No. 11, 1968, pp. 2090-2094.

[46] Dunn, M. G., "Measurement of $C^+ + e^- + e^-$ and $CO^+ + e^-$ Recombination in Carbon Monoxide Flows", *AIAA Journal*, Vol. 9, No. 11, 1971, pp. 2184-2191.

[47] Cohen, N. and Westberg, K. R., "Chemical Kinetic Data Sheets for High-Temperature Chemical Reactions", *Journal of Physical and Chemical Reference Data*, Vol. 12, No. 3, 1983, pp. 531-590.

[48] Millikan, R. C. and White, D. R., "Systematics of Vibrational Relaxation", *Journal of Chemical Physics*, Vol. 39, No. 12, 1963, pp. 3209-3213.